PHYSICAL REVIEW E **74**, 055201(R) (2006)

Frequency locking and complex dynamics near a periodically forced robust heteroclinic cycle

J. H. P. Dawes* and T. L. Tsai
DAMTP, Centre for Mathematical Sciences, University of Cambridge, Wilberforce Road, Cambridge, CB3 0WA, United Kingdom
(Received 18 July 2006; published 6 November 2006)

Robust heteroclinic cycles occur naturally in many classes of nonlinear differential equations with invariant hyperplanes. In particular they occur frequently in models for ecological dynamics and fluid mechanical instabilities. We consider the effect of small-amplitude time-periodic forcing and describe how to reduce the dynamics to a two-dimensional map. In the limit where the heteroclinic cycle loses asymptotic stability, intervals of frequency locking appear. In the opposite limit, where the heteroclinic cycle becomes strongly stable, the dynamics remains chaotic and no frequency locking is observed.

DOI: 10.1103/PhysRevE.74.055201 PACS number(s): 05.45.−a, 82.40.Bj

I. INTRODUCTION

The behavior that emerges out of cooperative or competitive interactions modeled by nonlinear differential equations is widely recognized to be difficult to predict and subtle to characterize. In the case of competitive interactions one might typically expect a single state to dominate after transients have decayed—the "winner-take-all" scenario. Recent work in game theory and evolutionary biology suggests that many scenarios are closer to a kind of "winnerless competition" rather than winner take all [1]. A standard example of winnerless competition is the playground game of rock-paper-scissors [2]. Dynamics due to winnerless competition has been inferred in many contexts, for example, the population dynamics of the lizard *Uta stansburiana* [3] and the dynamics of sensory neurons [4,5].

Mathematically, winnerless competition corresponds to the existence of a robust heteroclinic cycle in the state space. A *heteroclinic cycle* is a topological circle of saddle-type equilibria and connecting orbits; it is said to be *robust* if the topology survives under perturbations that preserve the flow invariance of the hyperplanes containing the connecting orbits. Robust heteroclinic cycles organize the dynamics in a wide range of systems: ecological models of competing species [6,7], thermal convection [8–11], intermittent bursts in boundary layers [12], coupled oscillator networks [13], and neurodynamics [5]. A detailed review of the mathematical theory and applications from many fields is given by Krupa [14]. Although robust heteroclinic cycles are well known in the symmetric dynamics literature [15,16] there appear to be very few discussions of the effects of time-periodic forcing, possibly only the papers [17,18].

An archetypal example of a robust heteroclinic cycle occurs in the following three-dimensional system, first studied for $\gamma=0$ by May and Leonard [7] and also by Busse and Heikes [9]:

$$\dot{x} = x(1 - X - cy + ez) + \gamma(1 - x)\sin^2 \omega t, \tag{1}$$

$$\dot{y} = y(1 - X - cz + ex), \tag{2}$$

$$\dot{z} = z(1 - X - cx + ey), \tag{3}$$

where $X=x+y+z$ and $c,e>0$. With the forcing term removed ($\gamma=0$) each of the equilibrium points on an axis is of saddle type, and the existence of connecting orbits has been proved by [19]. Moreover, if $c>e$ then the heteroclinic cycle is asymptotically stable. For higher-dimensional cycles stability turns out to be a subtle issue, and it is useful to define notions of stability that are weaker than asymptotic stability [20–23].

In this paper we examine the system (1)–(3), which is equivalent to the example studied by Rabinovich *et al.* [17], and answer two questions about the dynamics. First, how can the dynamics be reduced systematically to a dynamical system of lower dimension? And second, is the dynamics one dimensional and thus equivalent to a circle map? We emphasize that the results of our calculations are of far wider interest than the specific problem studied in [17] due to the ubiquity of robust heteroclinic cycles, and the importance of understanding the effects of different classes of perturbations.

In what follows we first discuss the construction of local and global maps that we compose to produce a two-dimensional (2D) return map to a Poincaré section; this answers the first question. We proceed to a show numerically that the dynamics of the two-dimensional return map is similar to a circle map if the ratio c/e is close to unity. Overall, there are important differences between the dynamics of (1)–(3) and the standard picture of frequency-locked periodic orbits, and Arnol'd tongues.

II. RETURN MAP

With the addition of small time-periodic forcing $0<\gamma\ll 1$, the invariant plane $x=0$ disappears. Trajectories of (1)–(3) are still, however, observed to spend long periods of time near the points $P_1=(1,0,0)$ which remains an equilibrium point, $P_2=(0,1,0)$, and $P_3=(0,0,1)$. These long periods are expected to be proportional to $\ln(1/\gamma)$ and are long compared to the rapid transitions between neighborhoods of the P_i. As in many problems of this type, this motivates an analysis based on splitting the dynamics into local behavior near the P_i and global maps between neighborhoods of the P_i (see Fig. 1).

*Electronic address: J.H.P.Dawes@damtp.cam.ac.uk; http://www.damtp.cam.ac.uk/user/jhd1002/

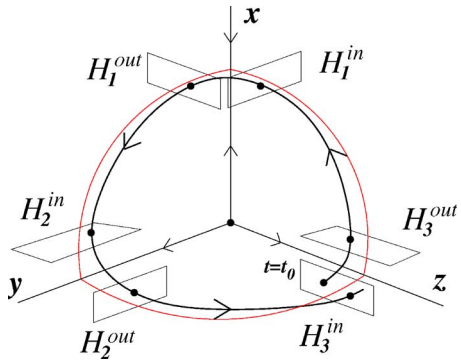

FIG. 1. (Color online) The arrangement of the Poincaré sections H_i^{in} and H_i^{out} transverse to a typical trajectory (thick line). The heteroclinic cycle for $\gamma=0$ is indicated by the thin (red) lines. For $\gamma\neq 0$ the plane $x=0$ is no longer flow invariant.

The local maps are given by analytical integration of the linearisation of (1)–(3) around each of the P_i. This is straightforward even when $\gamma\neq 0$. Near P_1 we integrate the linearization of (1)–(3) from the plane $H_1^{in}\equiv\{z=h\}$ to $H_1^{out}\equiv\{y=h\}$, and define H_2^{in}, H_2^{out}, H_3^{in} and H_3^{out} similarly. We compose these local maps with global maps from one neighborhood to another. The global maps are given, in the case $\gamma=0$, by linearizing around the unstable manifold of each of the P_i; thus they always introduce into the return map coefficients that are in principle computable (numerically), but which in practice are usually left undetermined since they do not affect the qualitative behavior of the return map. In the present case the problem is more severe since the global maps are time dependent. The global maps $P_1\to P_2$ and $P_3\to P_1$ in addition take into account the invariance of the planes $x_3=0$, and $x_2=0$, respectively. As long as h is small enough, the resulting return map does not depend on the value of h; we fix $h=0.2$. Full details of the construction will appear elsewhere.

Composition of the local and global maps, keeping only the leading order terms in the forcing amplitude γ, leads to a return map $H_3^{in}\to H_3^{in}$ of the form

$$x_{n+1}=\mu_1 x_n^d+\gamma\mu_2(1-a_1\cos 2\omega g_n-b_1\sin 2\omega g_n)+\gamma f(x_n,t_n), \tag{4}$$

$$t_{n+1}=g_n-\frac{\gamma\xi_2}{x_n}(1-a_2\cos 2\omega t_n+b_2\sin 2\omega t_n), \tag{5}$$

where we define x_n to be the x coordinate on H_3^{in} and t_n to be the time at which we arrive there. We also define $g_n=t_n+\mu_3-\xi_1\ln x_n$, $\xi_1=(e^2+ce+c^2)/e^3$, $\xi_2=(e^2+ce+c^2)/(2e^4)$, $a_1=c^2/(c^2+4\omega^2)$, $b_1=2c\omega/(c^2+4\omega^2)$, $a_2=e^2/(e^2+4\omega^2)$, $b_2=2e\omega/(e^2+4\omega^2)$, and $d=(c/e)^3$. We assume $d>1$ since otherwise the heteroclinic cycle is unstable in the absence of forcing, and trajectories move rapidly away from it. As discussed above, the coefficients μ_1,μ_2,μ_3 and the function $f(x_n,t_n)$ arise from the global maps and are undetermined by the reduction procedure, although they are in principle computable numerically. Importantly, these coefficients, and $f(x_n,t_n)$, depend on ω; determining the dependence on ω is a crucial part of producing a quantitatively accurate return map. We now discuss the behavior of (4) and (5) in the limits of large and small ω.

In the limit $\omega\to\infty$ the effect of the forcing term on trajectories is given by the averaged value $\frac{1}{2}\gamma(1-x)$. A perturbed heteroclinic cycle usually produces a nearby periodic orbit, i.e., a fixed point for (4) and (5). Suppose that in the limit $\omega\to\infty$ the function $f(x_n,t_n)$ tends to a constant C_0. Then, assuming $d\gg 1$ we approximate (4) by $x=\gamma(\mu_2+C_0)$; from (5) the period of the periodic orbit $T=t_{n+1}-t_n$ is given approximately by

$$T=\mu_3-\xi_1\ln\gamma(\mu_2+C_0)-\frac{\xi_2}{C_0}\equiv C_1-\xi_1\ln\gamma. \tag{6}$$

Comparison with numerical integrations (not shown) shows that the relationship between T and $\ln\gamma$ very closely follows (6); we find $C_1=-32.4$ for $(c,e)=(0.25,0.2)$, and this provides direct confirmation of the return map calculation. Note that the dashed lines in Fig. 5 also confirm the expression for the slope ξ_1.

For small ω we fix a functional form for $f(x_n,t_n)$ and fit the coefficients μ_i to the dynamics of the ordinary differential equations (ODEs) for one particular set of parameter values: $c=0.25$, $e=0.2$, $\gamma=10^{-6}$. We show in the next section that this single set of coefficients describes the dynamics over a range of values of c, not just for the value $c=0.25$ used in the fitting process. We take $f(x_n,t_n)$ in the form

$$f(x_n,t_n)=\mu_2 a_1(1-\mu_4)\cos 2\omega g_n+\frac{1}{2}(\mu_5+\mu_6 a_1\omega+\mu_7 a_1^2\omega^2), \tag{7}$$

and fix the coefficients $\mu_1,\ldots,\mu_7$ for the remainder of the paper to take the values $\mu_1=1$, $\mu_2=26.8$, $\mu_3=52$, $\mu_4=2.42$, $\mu_5=70$, $\mu_6=200$, $\mu_7=12\,300$. Figure 2 shows that excellent, and detailed, agreement over the range $0\leqslant\omega\leqslant 0.1$ is obtained between numerical integrations of the ODEs and the 2D map.

III. RESULTS AND DISCUSSION

We have compared the results of integrating the ODEs (1)–(3) and iterating the map (4) and (5) for several collections of parameter values (c,e,γ), without adjusting the coefficients in (7); these results confirm that the map remains accurate over a wide range of parameter space. By way of illustration, Fig. 3 compares the results of the ODEs and the map for $c=0.205$; there is very good agreement without adjustment of the parameters $\mu_1,\ldots,\mu_7$.

The general features of the dynamics are a sequence of frequency-locking intervals within which there is a stable periodic orbit of period $T=k\pi/\omega$ for integer k. Thus the curved lines in Figs. 2 and 3 lie on hyperbolas indexed by k. Within these intervals there are sometimes subintervals where the periodic orbit undergoes a period-doubling bifurcation. At the ends of the frequency-locking intervals the periodic orbit disappears in a saddle-node bifurcation; this is confirmed by plotting t_{n+1} against t_n for fixed ω (see Fig. 4).

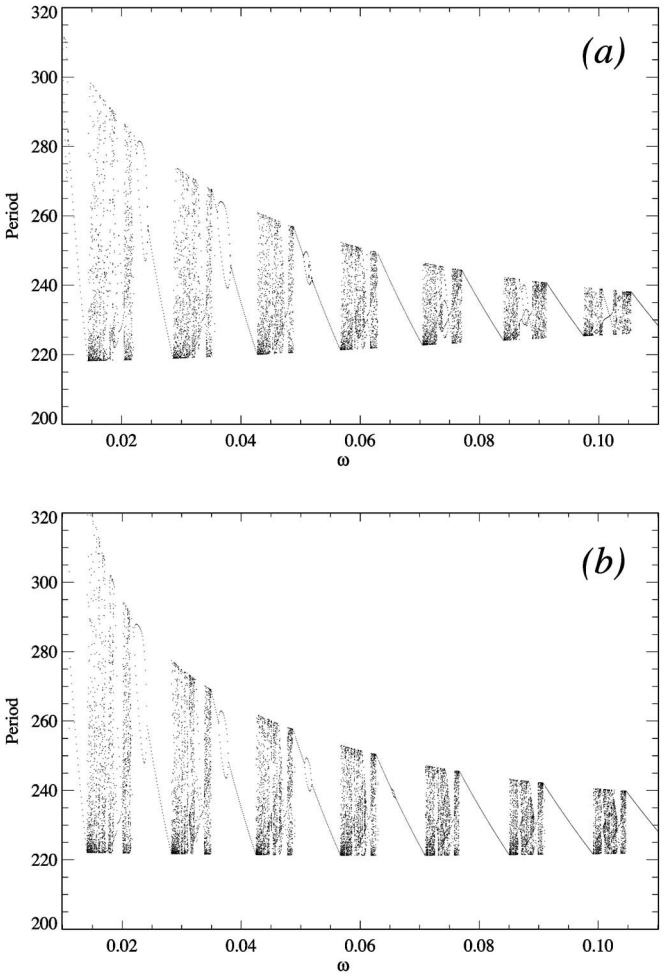

FIG. 2. (a) Period T of trajectories of the ODEs (1)–(3) returning to H_3^{in} as a function of ω, after transients have decayed. Parameters: $c=0.25$, $e=0.2$, $\gamma=10^{-6}$. Line segments indicate frequency locking resulting in a periodic orbit with period $k\pi/\omega$ for successive integers k. (b) Period $t_{n+1}-t_n$ for iterates of the 2D map (4) and (5).

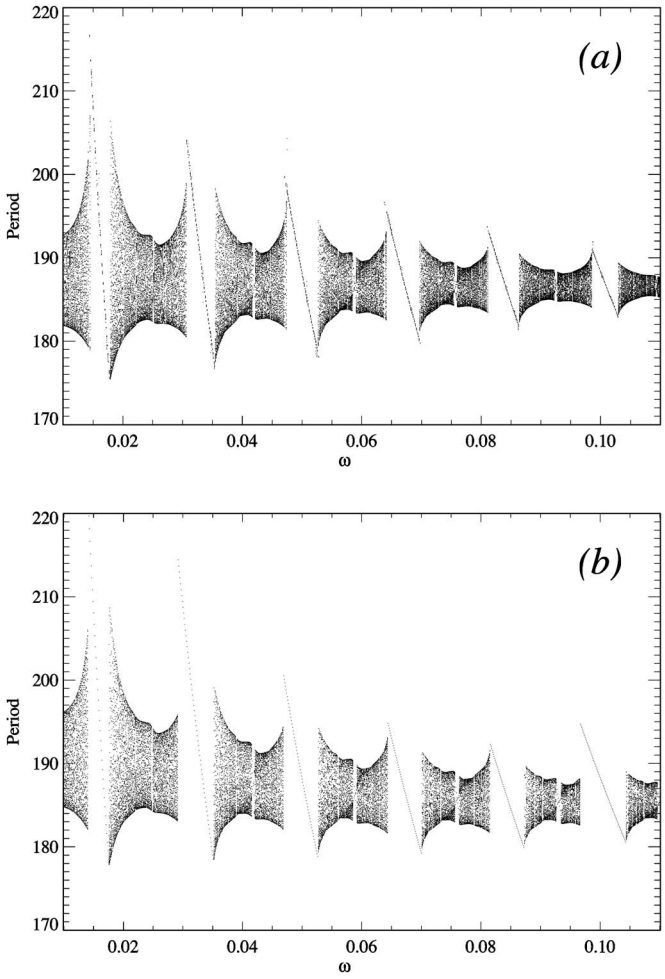

FIG. 3. (a) Period T of trajectories of the ODEs (1)–(3) returning to H_3^{in} as a function of ω. Parameters: $c=0.205$, $e=0.2$, $\gamma=10^{-6}$. (b) Period $t_{n+1}-t_n$ for iterates of the 2D map (5) and (7).

More precisely, in this figure we plot $t_n \bmod \pi/\omega$ since the 2D map is periodic in t_n. The figure shows that the 2D map has essentially one-dimensional dynamics; this supports, at least for $c=0.25$, the natural hypothesis of circle map-like dynamics.

Figure 5 illustrates the scaling of the bifurcation structure with γ. The dashed lines in Fig. 5 take the form $y=-1-k\pi/(\omega\xi_1 \ln 10)$ for $k=1,\ldots,4$ showing the scaling of the intervals of frequency locking (the factor of $\ln 10$ is needed only because of the $\log_{10}$ used on the vertical axis). Note also the repeated appearance of new windows of period-doubled orbits at small $1/\omega$ as γ decreases.

For c/e close to unity the dynamics of the 2D map appear close to those of a circle map; the curve in the plot corresponding to Fig. 4 is monotonically increasing and becomes linear for c/e very close to unity. Further numerical results, not shown here, indicate that the widths of the frequency-locking intervals do not tend to zero rapidly as $c/e \to 1^+$.

Figure 6, reminiscent of the Hénon map, illustrates the case $c=1.0$. For $c=1.0$ the cycle is strongly attracting in the absence of forcing. But in the presence of forcing, the dynamics of the map, and also of the original ODEs, are clearly far from one-dimensional; we observe that c/e large enhances the nonlinearity present in the 2D map.

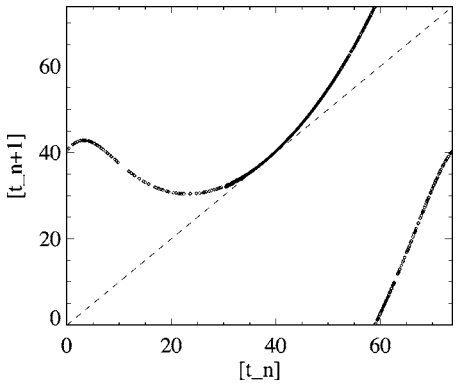

FIG. 4. Circle-map-like dynamics: $[t_n]$ against $[t_{n+1}]$ where $[t_n] \equiv t_n \bmod \pi/\omega$, for $\omega=0.042\,58$. This corresponds to a saddle-node bifurcation point at the end of an interval of frequency locking. Other parameter values are as for Fig. 2: $c=0.25$, $e=0.2$, $\gamma=10^{-6}$.

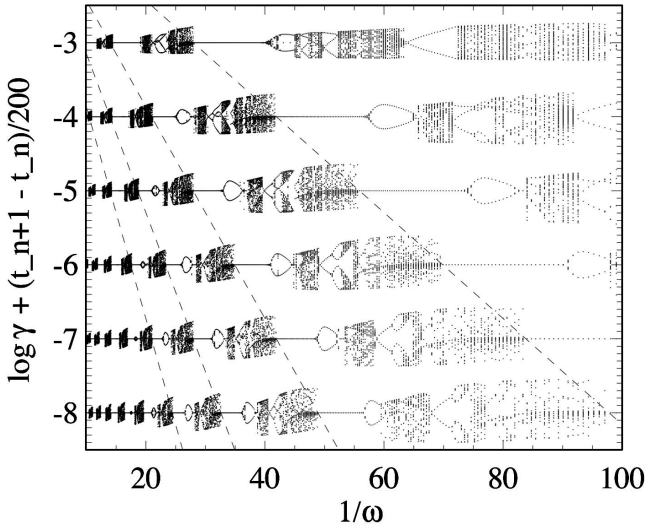

FIG. 5. Bifurcation structure scaling with γ. $\log_{10}\gamma + (t_{n+1}-t_n)/200$ (vertical axis) plotted against $1/\omega$ (horizontal axis), for $\gamma=10^{-n}$, $3\leqslant n\leqslant 8$. Other parameter values are as for Fig. 2: $c=0.25$, $e=0.2$.

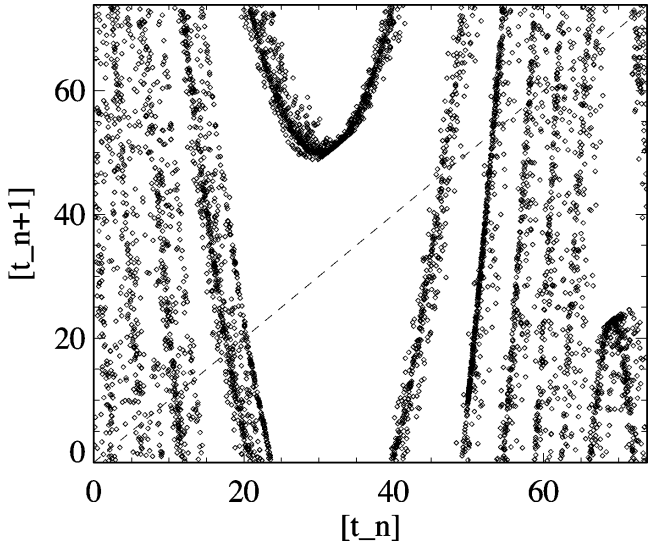

FIG. 6. Complex dynamics in the map (5)–(7) for $c=1.0$. Other parameter values are $\omega=0.042\,58$, $e=0.2$, and $\gamma=10^{-6}$.

In conclusion we have presented a careful and quantitatively accurate analysis of the dynamics of a robust heteroclinic cycle subjected to time-periodic forcing. The dynamics are well described by a two-dimensional map over a wide range of the eigenvalue ratio c/e. In the limit $c/e\to 1^+$ the dynamics exhibits a sequence of frequency-locking windows which often contain smaller period-doubling windows, and intervals of chaotic dynamics; this behavior is similar to the dynamics of a circle map. In the limit $c/e\gg 1$ there are no windows of frequency locking and the dynamics is chaotic for all ω. These aspects of the dynamics are puzzling at first sight, and we intend to pursue them further and report detailed results in future.

Since the form of the forcing breaks both the permutation symmetry and the invariance of the $x=0$ plane in (1)–(3), dynamics similar to that which we have described is expected to occur generically near periodically forced robust heteroclinic cycles.

ACKNOWLEDGMENTS

T.L.T. acknowledges financial support from the Government of Taiwan and the Cambridge Overseas Trust.

[1] M. A. Nowak and K. Sigmund, Science **303**, 793 (2004).
[2] M. Frean and E. R. Abraham, Proc. R. Soc. London, Ser. B **268**, 1323 (2001).
[3] B. Sinervo and C. M. Lively, Nature (London) **380**, 240 (1996).
[4] M. Rabinovich, A. Volkovskii, P. Lecanda, R. Huerta, H. D. I. Abarbanel, and G. Laurent, Phys. Rev. Lett. **87**, 068102 (2001).
[5] P. Varona, R. Levi, Y. I. Arshavsky, M. I. Rabinovich, and A. I. Selverston, Neurocomputing **58–60**, 549 (2004).
[6] J. Hofbauer and K. Sigmund, *Evolutionary Games and Population Dynamics* (Cambridge University Press, Cambridge, U.K., 1998).
[7] R. M. May and W. Leonard, SIAM J. Appl. Math. **29**, 243 (1975).
[8] D. Armbruster, J. Guckenheimer, and P. Holmes, Physica D **29**, 257 (1987).
[9] F. H. Busse and K. E. Heikes, Science **208**, 173 (1980).
[10] R. M. Clever and F. H. Busse, J. Fluid Mech. **94**, 609 (1979).
[11] M. R. E. Proctor and C. A. Jones, J. Fluid Mech. **188**, 301 (1988).
[12] P. Holmes, J. L. Lumley, and G. Berkooz, *Turbulence, Coherent Structures, Dynamical Systems and Symmetry* (Cambridge University Press, Cambridge, U.K., 1996).
[13] A. S. Kuznetsov and J. Kurths, Phys. Rev. E **66**, 026201 (2002).
[14] M. Krupa, J. Nonlinear Sci. **7**, 129 (1997).
[15] P. Chossat and R. Lauterbach, *Methods in Equivariant Bifurcations and Dynamical Systems* (World Scientific, Singapore, 2000).
[16] M. J. Field and J. Swift, Nonlinearity **4**, 1001 (1991).
[17] M. I. Rabinovich, R. Huerta, and P. Varona, Phys. Rev. Lett. **96**, 014101 (2006).
[18] M. Tachikawa (unpublished).
[19] J. Guckenheimer and P. Holmes, Math. Proc. Cambridge Philos. Soc. **103**, 189 (1988).
[20] M. Krupa and I. Melbourne, Ergod. Theory Dyn. Syst. **15**, 121 (1995).
[21] M. Krupa and I. Melbourne, Proc. R. Soc. Edinburgh, Sect. A: Math. **134**, 1177 (2004).
[22] C. M. Postlethwaite and J. H. P. Dawes, Nonlinearity **18**, 1477 (2005).
[23] I. Melbourne, Nonlinearity **4**, 835 (1991).